

New Hysteresis Control Method for Three Phase Shunt Active Power Filter

Mohamed R. Amer, Osama A. Mahgoub, Sherif A. Zaid

Abstract—The quality of the current waveform generated by a current controlled, voltage source shunt active power filter depends basically on three factors: (i) The reference signal being generated; (ii) the modulation method used and (iii) the switching frequency of the PWM modulator. A new adaptive hysteresis band modulation method is proposed. In this paper, the periodical sampling constant hysteresis band modulation method and the proposed method are analyzed. These modulation methods are tested in switching an active power filter based on a voltage source topology, in a three phase three wire connections. They are compared in terms of THD of supply current, switching losses, and their flexibility of tuning. The simulation results demonstrate the viability and effectiveness of the new adaptive Hysteresis band modulation method in reducing the ripple, losses, and THD of supply current.

Index Terms - Voltage Source Inverter (VSI), Active Power Filter (APF), Hysteresis Modulation Technique.

I. INTRODUCTION

The performance requirements of active power filters (APF) are hardly met by digital controls slowed down by conversion delays and calculation times. Fast transients and high current-harmonic content call for wide-band controls. To obtain high accuracy and to compensate for the voltage disturbances a high loop gain must be adopted. However, a safe stability margin must be ensured too.

The above requirements conflict with each other. The performance can be improved by increasing the switching frequency. However, as in active filters, the power involved is quite high and the available switching components do not allow too high frequencies to be adopted. Moreover, as the switching frequency increases, the effects of the dead times increase as well, which add to the voltages disturbances mentioned above.

Manuscript received December 08, 2010; revised December 22, 2010.

Mohamed R. Amer is a lecturer assistant in department of Electrical power and Machines, Faculty of Engineering, Cairo University, Egypt. (Phone: 0020123318931; e-mail: m_rabah83@yahoo.com).

Osama A. Mahgoub is a Professor in department of Electrical power and Machines, Faculty of Engineering, Cairo University, Egypt. (Phone: 0020235678935; e-mail: mahgoub04@yahoo.com).

Sherif A. Zaid is a lecturer in department of Electrical power and Machines, Faculty of Engineering, Cairo University, Egypt. (Phone: 0020235678935; e-mail: sherifzaid@yahoo.com).

A satisfactory solution for these requirements has proven to be the hysteresis current-control technique, which is characterized by unconditioned stability, fast response, and good accuracy. Although this technique is essentially an analog one, it has been shown that the major part of its implementation can be done by digital means, thus obtaining several of the advantages typical of digital solutions.

The hysteresis band is used to control the supply current and determine the switching signals for inverters gates. When the supply current exceeds the upper band, the comparators generate control signals in such a way to decrease the supply current and keep it between the bands.

The basic hysteresis technique is affected by the drawbacks of a variable switching frequency and of a heavy interference among the phases in the case of a three-phase system with isolated neutral. Effective methods to eliminate these inconveniences have been introduced some time ago and have been demonstrated to be a viable way to obtain robust and high-performance controls. Additional improvements were proposed [1, 2] to give the system the ability to ensure pulse-phase control to minimize the ripple contents, similarly to the optimal pulse position produced by the vectorial techniques [3].

In this paper, a further and substantial improvement of the hysteresis control is proposed, which is characterized by a very simple and robust implementation. It offers all the advantages of the hysteresis technique.

II. THREE PHASE SHUNT APF MODEL

The shunt APF is a device that is connected parallel to compensate the reactive power and to eliminate harmonics from non-linear loads.

The scheme of the APF considered in this paper is presented in Fig.1. It is a three-phase converter, where the capacitor is the main energy storage element and the inductors are used for the control of the filter currents by means of the converter voltages.

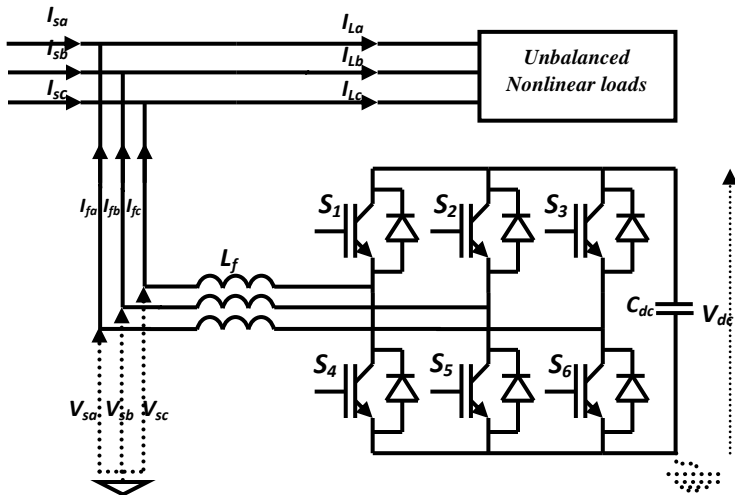


Fig. 1 Fundamental building block of the active filter

Applying Kirchoff's laws for the currents and the voltages at the connection point of the shunt APF leads to the following equations in the "abc" frame [4, 5]:

$$\begin{aligned}
 L_f \frac{di_{fa}}{dt} &= V_{sa} - d_n V_{dc} \\
 L_f \frac{di_{fb}}{dt} &= V_{sb} - d_n V_{dc} \\
 L_f \frac{di_{fc}}{dt} &= V_{sc} - d_n V_{dc}
 \end{aligned} \tag{1}$$

Where d_{nk} "the switching state function" can be defined as:

$$\begin{pmatrix} d_{n1} \\ d_{n2} \\ d_{n3} \end{pmatrix} = \frac{1}{3} \begin{pmatrix} 2 & -1 & -1 \\ -1 & 2 & -1 \\ -1 & -1 & 2 \end{pmatrix} \begin{pmatrix} C_1 \\ C_2 \\ C_3 \end{pmatrix} \tag{2}$$

Switching function C_k of the k^{th} inverter leg ($k = 1, 2, 3$), which is defined as, follows:

$$C_k = \begin{cases} 1, & \text{if } S_k \text{ is on and } S_{k+3} \text{ is off} \\ 0, & \text{if } S_k \text{ is off and } S_{k+3} \text{ is on} \end{cases}$$

III. CONTROL ALGORITHM FOR APF

In this paper, a simple Synchronous reference frame (SRF)-based scheme is used to extract positive sequence fundamental frequency active current from non-linear unbalanced loads currents.

The control scheme for the proposed system is based on the SRF based current decomposition. Figure 2 shows the flow of various control signals and control scheme based on the decomposed components. The control scheme depicted in Fig.2 also incorporates the command for maintaining the constant average DC bus voltage at the VSI.

A PI controller is used also to regulate the DC bus voltage to its reference value and compensates for the inverter losses. A low pass filter is used to filter the ripples in the feedback path of the DC link voltage. The filtering of DC voltage ensures that power transfer between the DC bus of the inverter and supply takes place only at fundamental frequency and not as a result of harmonic frequency. To compensate the inverter losses and maintaining the DC bus voltage, the demanded current is added to positive sequence fundamental frequency component of load current, as shown in the Fig. 2.

The PWM gating pulses for the IGBTs in VSI of APF are generated by indirect current control using hysteresis current controller over reference supply currents (i_{sa}^* , i_{sb}^* , i_{sc}^*) and sensed supply currents (i_{sa} , i_{sb} , i_{sc}). The controlled compensation current is injected such that the supply current follows the reference current. Hence the source current becomes close to reference currents estimated by SRF decomposer.

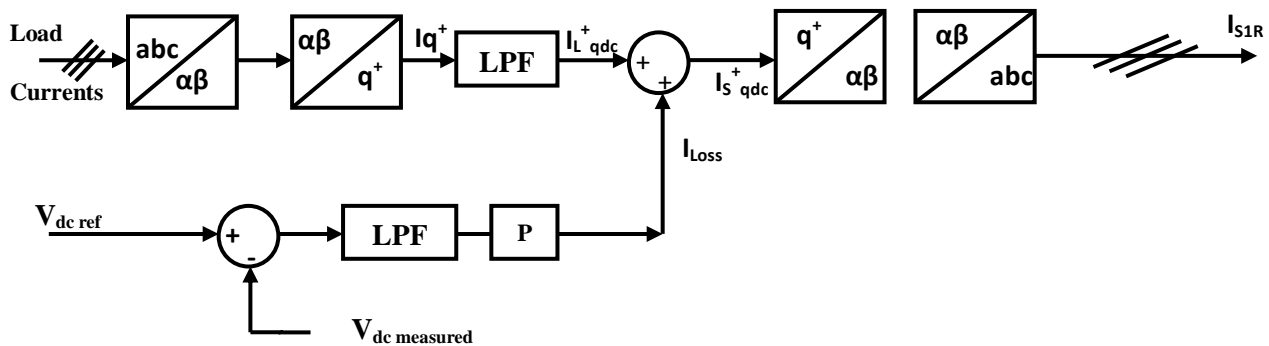


Fig.2 Control scheme for APF

IV. MATLAB BASED SIMULATION

The power supply, rectifier with resistive load, unbalanced load and APF is modeled in MATLAB using Power System Block set. Figure 3 depicts the test bench to estimate the performance of the APF with proposed control scheme. The source block consists of three-phase voltage source with small impedance representing a stiff source to gauge the performance of the APF with proposed scheme. The set of load consists of diode rectifier and delta connected resistive load with unequal arm. The rectifier fed load has been modeled as diode rectifier feeding resistance, which represents the real power consumed by the load. The unbalance in the load current has been generated by three phase delta connected resistive load.

The simulation results have been studied for computing the performance of APF with two modulation methods by analysis through THD of supply current.

The Shunt APF consists of two main parts: a) The Inverter, b) The controller. The controller is fed with the measurements from the main system in addition with the inverter currents and the voltage of the DC side of the inverter. It produces the switching scheme of the switches (IGBT's) of the inverter. Also, it gives the signal required for the initial charging of the capacitor in the DC side of the inverter.

The inverter consists of three parallel modules; each consists of two IGBT's connected in series with their anti-parallel diodes. The DC side is a capacitor bank (C=900µF).

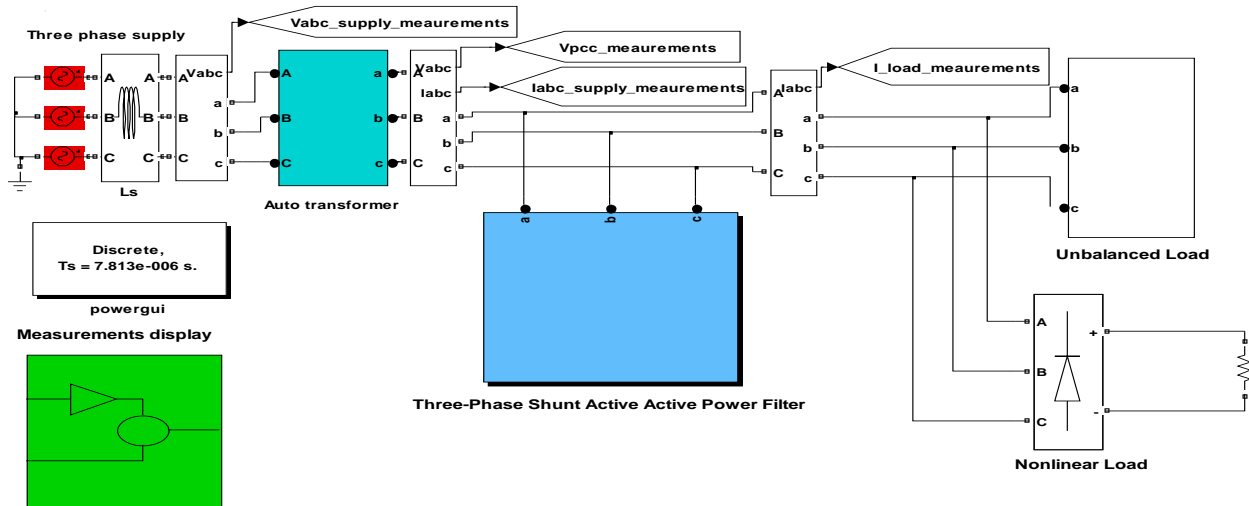


Fig.3 Main block of proposed control scheme with APF under MATLAB

V. PERIODICAL SAMPLING CONSTANT HYSTERESIS BAND MODULATION METHOD

The PWM switching of VSI devices is described as follows:

If $I_{act} > (I_{ref} + hb)$ upper switch of leg is ON and lower switch is OFF.

If $I_{act} < (I_{ref} - hb)$ upper switch of leg is OFF and lower switch is ON.

The capacitor bank is first charged from the main system supply through the charging resistance ($R=15\Omega$) and the diodes acting as an uncontrolled rectifier bridge. After the initial charging of the DC capacitors, when the voltage on the capacitor reaches certain value “230V”, this resistance is short circuiting by a contactor. Also, a line inductor is used at the output of each module in order to smooth the inverter current. Forward voltages of IGBT devices and diodes are 2.8V and 1V respectively. The switching times of IGBT are 3µs. Table I presents the parameters of the simulated system.

TABLE I
THE PARAMETERS OF THE SIMULATED SYSTEM

Total Line impedance	$L_s=0.733 \text{ mH}, R_s=0.1\Omega$
Unbalanced delta connected load	$R_{ab}=67\Omega, R_{cb}=R_{ca}=135\Omega$
Non-linear load(rectifier with R_{dc})	$R_{dc}=20\Omega$
Coupling Impedance	$L_f=2\text{mH}, R_f=1.0\Omega$
Dc bus voltage	400V
Max switching frequency	12.8kHz
Hysteresis band(Hb)	0.4A
Dead time	8µs
Line frequency	50Hz
Mains voltage per phase	100V

It must be noted that there is a delay time must be considered in the simulation system of APF. This time is used by the digital control system to obtain the system voltages and currents via transducers, to sample the currents and voltages, and to convert the signal back to analogue signal (driving signal). This time is set to be 15µsec.

Where, hb is the hysteresis band around the reference current I_{ref} . Number of samples over a cycle has been held constant at 256. The loop time thus become nearly fixed at $78.125\mu s$ to realize a max possible frequency of hysteresis controller at 12.8 kHz. A dead time of $8\mu s$ is set between upper and lower devices of a leg of the VSI to avoid the short circuit. The hysteresis control method is simple to be implemented, and its dynamic performance is excellent. There are some inherent drawbacks, though [6-9]:

- i. There is no intercommunication between the individual hysteresis controllers of the three phases and hence no strategy to generate zero voltage vectors. This increases the switching frequency at lower modulation index.
- ii. There is a tendency at lower speed to lock into limit cycles of high-frequency switching which comprise only nonzero voltage vectors.
- iii. The current error is not strictly limited. The signal will leave the hysteresis band whenever the zero vector is turned on while the back-emf vector has a component that opposes the previous active switching state vector. The maximum overshoot is Δi .

Figure 4 shows the ripple in the APF generated current.

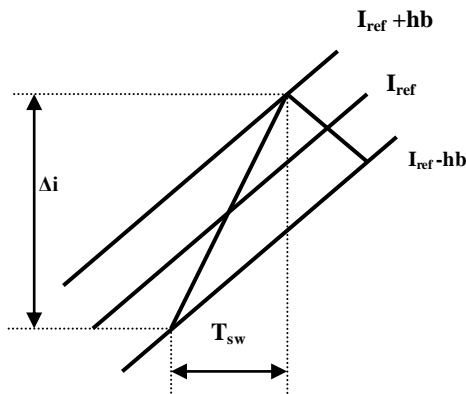


Fig.4 Ripple in the APF generated current

Using the modeling equations of VSI as an APF (equations 1 and 2), factors that affect the ripple in APF generated current can be deduced.

From the previous figure, the slope of the generated APF current (di/dt) can be calculated:

$$di / dt = \Delta i / T_{sw} \quad (3)$$

And the rate of change of the generated current (di/dt) is dependent on the instantaneous supply voltage as shown in the following equation:

$$L di / dt = V_s - d_{nk} V_{dc} \quad (4)$$

Figure 5 shows the block diagram of the hysteresis modulation technique. This technique is called periodical sampling constant hysteresis band. This method is very simple to be implemented and the actual frequency is not

clearly defined but it is limited by the sampling clock. Figure 6 shows the reference current with constant hysteresis band. Figures 7 and 8 show the simulation results for both load and supply currents respectively for constant hysteresis band modulation.

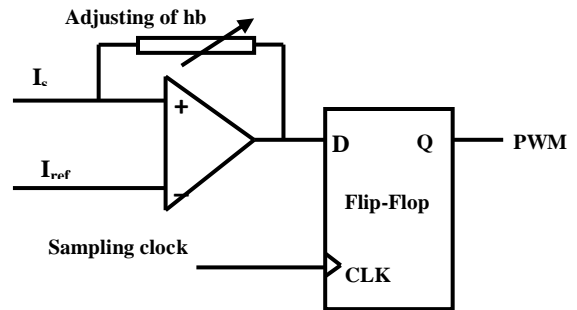


Fig.5 Block diagram of periodical sampling constant Hysteresis band

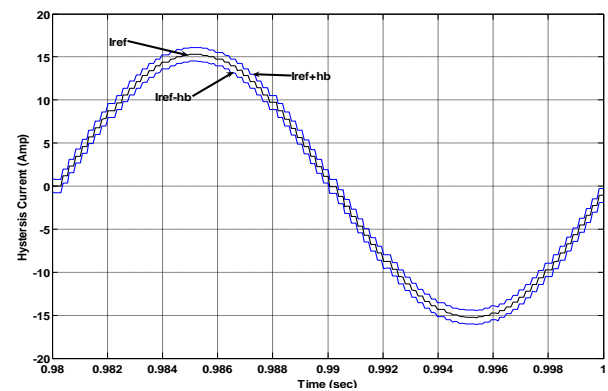


Fig.6 Reference current with constant Hysteresis band

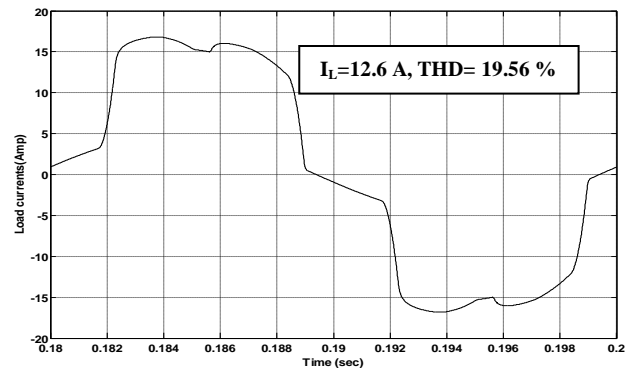


Fig.7 Load current

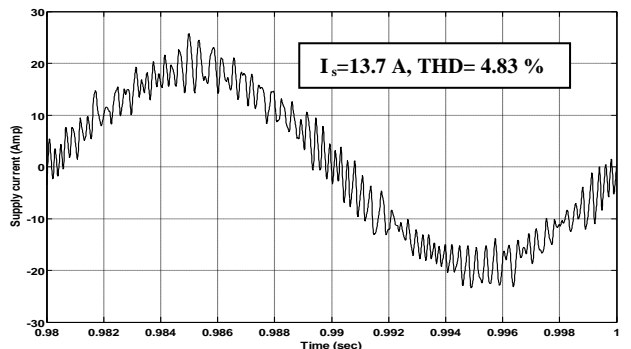


Fig.8 Supply current for constant Hysteresis band

It is noticed, in Fig. 8, the high ripple presented in supply currents. The expressions of the ripple in the current, equations 3 and 4, show that the current ripple increases when the switching frequency and/or the reactor value decreases. Also, the current ripple increases when the dc bus voltage increases. Moreover, the current ripple also affects THD especially in low currents. In previous simulation the supply current is 13.8 Amp.

Also, in constant band periodical sampling, the generated current does not swing symmetrically around the reference signal: it has a biasing error.

VI. NEW ADAPTIVE HYSTERESIS BAND MODULATION METHOD

The hysteresis modulator is modified to reduce the switching losses by applying variable frequency; to make the generated current swing symmetrically around the reference signal with minimum possible ripple, and to adapt the hysteresis band for any current.

The generated current can be forced to symmetrically swing around the reference signal by making constant ripple among the whole cycle. The ripple of the generated current is dependent on different factors such as: instantaneous supply voltage, dc bus voltage, coupling inductor, and the switching time. The only controlled variable from these factors is the switching time. The switching time can be controlled by changing the hysteresis band.

The generated current has its maximum slope at the peak of the supply voltage. On the other hand, the reference signal is in phase with the supply voltage and so, its slope is minimum value at the peak of the supply voltage. This high difference in the rate of change between the generated current and the reference current leads to high unsymmetrical ripple at this instant. To reduce this ripple, the PWM signal can be forced to track the rate of generated current to make it closer to the reference current. As well as, the generated current has its minimum slope and the reference signal has its maximum slope at the minimum of the supply voltage. But $(di/dt)_{APF}$ is higher than $(di/dt)_{ref}$ at any moment. At this instant the generated and reference currents are very close to each other. So, PWM modulator can be forced to wait for certain difference between the reference and the generated current. In other words, the new modification of the modulator force the PWM signals to turn on the IGBT devices with high switching frequency (low switching time) at the peak of the reference current and with low frequency (high switching time) at minimum of the reference current.

The switching frequency of the PWM signals for periodical sampling system can be controlled by the tuning of hysteresis band. And this achieved by making low Hysteresis band at reference current maximum and high Hysteresis band

at reference current minimum. Figure 9 and 10 show the block diagram of adaptive hysteresis band controller and the relation between Hysteresis band and the reference current.

The dependence of the Hysteresis band on the rate of change of the reference current achieves two goals; the first goal is varying the Hysteresis band around the cycle with minimum value at peak reference current and maximum value at minimum reference current. The second goal is self tuning of Hysteresis band with any value of current with no need to re-adjust the Hysteresis band. Figure 11 shows the reference current with the new adaptive Hysteresis band.



Fig.9 Block diagram of adaptive Hysteresis band

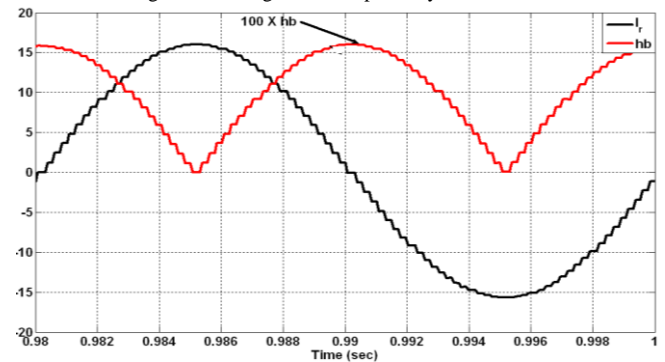


Fig.10 Relation between adaptive Hysteresis band and reference current

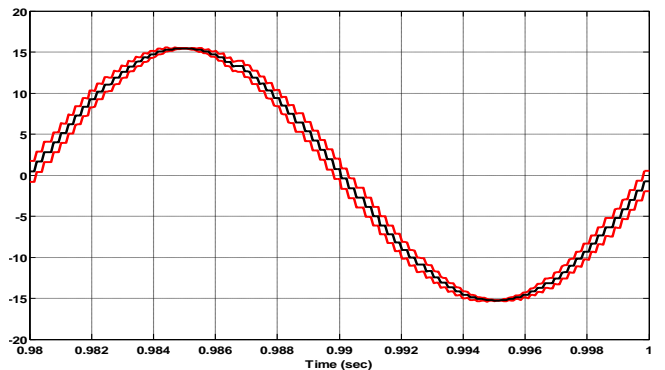


Fig.11 Reference current with adaptive Hysteresis band

Figures 12 and 13 show the switching pulses of the constant hysteresis band and the new modulation method.

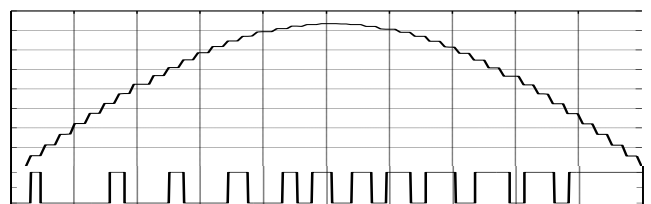


Fig.12 Switching pulses for constant hysteresis band

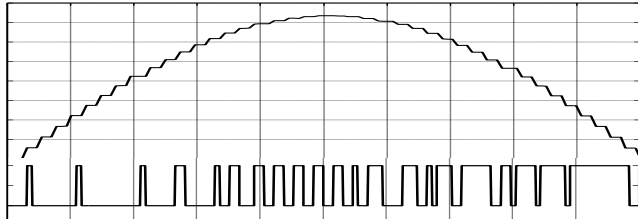


Fig.13 Switching pulses for adaptive hysteresis band

It can be seen the switching frequency, in constant hysteresis band, is almost constant around the half cycle of reference current. On the other hand, the switching frequency, in new adaptive method, is high at maximum reference current and is low at minimum reference current. Figures 14 shows the supply current for new adaptive hysteresis band.

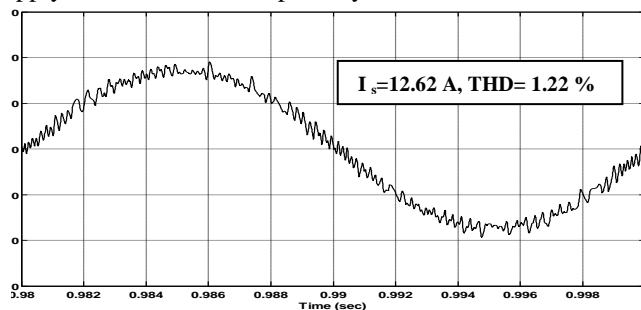


Fig.14 Supply current for new adaptive Hysteresis band

TABLE II
COMPENSATION RESULTS OF APF

Sampling time (Ts)		THD %			RMS supply currents		
		"a"	"b"	"c"	"a"	"b"	"c"
78.125μs	Without APF	19.56	19.66	21.63	12.6	12.65	11.4
	Constant Hb	4.83	4.89	3.23	13.7	13.8	13.8
	Adaptive Hb	1.22	1.68	1.59	12.62	12.62	12.65
15.625μs	Constant Hb	1.62	1.69	1.4	13.5	13.53	13.54
	Adaptive Hb	0.54	0.63	0.56	12.39	12.37	12.38

The previous figures show the improvement in supply current waveform with new adaptive Hysteresis band and reducing of ripple current without increasing the maximum switching frequency. Table II shows the compensation results of APF for both constant and adaptive hysteresis band modulation method.

It can be seen the great effect of adaptive Hysteresis band in enhancement the performance of APF especially in reducing the THD and rms values of supply currents.

The test of the proposed system, with all the same system parameters, is repeated with the rectifier loaded by $R_{dc}=5\Omega$. Table III shows the simulation results of higher load currents for both the constant and adaptive hysteresis band. For constant hysteresis band, the band should be retuned for the new value of current. But in adaptive hysteresis band, there is no need for re-adjusting.

TABLE III
COMPENSATION RESULTS OF APF FOR HIGHER SUPPLY CURRENT

	THD %			RMS supply currents		
	"a"	"b"	"c"	"a"	"b"	"c"
Without APF	21.46	21.61	22.24	38	37.96	38.2
Constant Hb	4.38	4.18	3.07	41.9	42	41.9
Adaptive Hb	3.29	3.49	3.25	41.1	41.3	41.3

VII. CONCLUSION

The characteristics of a new adaptive hysteresis band modulation method are analyzed, tested, and compared with the used constant hysteresis band modulation in terms of THD of supply current and their flexibility of tuning.

The simulation results demonstrate the viability and effectiveness of the new adaptive Hysteresis band in reducing the ripple, losses and THD of supply current. The new adaptive method relates the Hysteresis band with the rate of change of the reference current. The dependence of the hysteresis band on the rate of change of the reference current achieves two goals. The first goal is varying the hysteresis band around the cycle with minimum value at peak reference current and maximum value at minimum reference current and so, controlling the switching time and switching frequency. The second goal is self-tuning of hysteresis band with any value of current with no need to re-adjust the Hysteresis band.

REFERENCES

- [1] L. Malesani, P. Mattavelli, and P. Tomasin, "Improved constant frequency hysteresis current control of VSI inverters with simple feed forward bandwidth prediction," in IEEE IAS Annu. Meet. Conf. Rec., Orlando, FL, Oct. 1995, pp. 2633–2640
- [2] L. Sonaglioni, "Predictive digital hysteresis current control," in IEEE IAS Annu. Meet. Conf. Rec., Orlando, FL, Oct. 1995, pp. 1879–1886.
- [3] H. W. Van der Broeck, H. C. Skudelny, and G. V. Stanke, "Analysis and realization of a pulse width modulator based on voltage space vectors," IEEE Trans. Ind. Appl., vol. 24, pp. 142–150, Jan./Feb. 1988.
- [4] S. Bhattacharya and D. M. Divan, "Synchronous frame harmonic isolator using active series filter," in Proc. EPE, pp. 3030-3035, 1991.
- [5] B. Singh, A. Chandra, and K. Al-Haddad, "Computer-aided modeling and simulation of active power filters," Elect. Mach. Power Syst., vol. 27, pp. 1227-1241, 1999.
- [6] D. M. Brod and D. W. Novotny, "Current control of VSI PWM Inverters," IEEE Trans. Industry Appl., Vol. IA-21, No. 3, pp. 562-570, May/June 1985.
- [7] S. Salama, S. Lennon, "Overshoot and Limit Cycle Free Current Control Method for PWM Inverter," EPE Europ. Conf. Power Electronics and Appl., Florence/Italy, 1991, pp. 3/247-251.
- [8] J. Rodriguez and G. Kastner, "Nonlinear Current control of an inverter-fed induction machine," ETZ Archiv, 1987, pp. 245 - 250.
- [9] L. Malesani and P. Tenti, "Novel hysteresis control method for current-controlled VSI-PWM inverters with constant modulation frequency," IEEE Ind. Appl. Soc. Ann. Meet., 1987, pp. 851 - 855.